

## Characteristic X-Ray Production in the $L_{III}$ Shell of Copper by Low-Energy (100- to 500-keV) Protons\*

J. M. KHAN, D. L. POTTER, AND R. D. WORLEY

Lawrence Radiation Laboratory, University of California, Livermore, California

(Received 22 November 1963)

Characteristic  $L$ -shell x rays produced when protons of 100- to 500-keV energy are stopped in thick targets of copper have been studied using proportional counter detection. As a consequence of self-absorption in the  $L_{II}$  and  $L_{III}$  shells, the relative intensities of the various  $L$  lines change with depth of penetration (hence energy) of the protons. By use of additional copper absorbers, lines originating from the filling of vacancies in the  $L_{III}$  shell can be isolated. [A single-crystal (KAP) spectrometer was used to verify this for electron-excited spectra.] Presented here are the thick-target yields for the  $L_{III}$  lines and the highly self-absorbed lines as well as the x-ray production cross section for the  $L_{III}$  lines. With a fluorescent yield of 0.05, the ionization cross section ( $\sigma_I = 3.6 \times 10^{-22}$  cm) at 100 keV is approximately two orders of magnitude lower than the value predicted on the basis of the Born approximation description of the proton trajectory.

### I. INTRODUCTION

CHARACTERISTIC x-ray production by proton bombardment has been studied by a number of investigators.<sup>1-9</sup> The method employed here involves the measurement of the thick-target yield as a function of proton energy. From this thick-target yield, knowledge of the stopping power of the material for the protons and the mass-absorption coefficient of the material for its own characteristic x rays, it is possible to obtain the x-ray production cross section. By correcting this cross section for the radiationless reorganization of the atom, the ionization cross section for the shell considered can be obtained.

In the case considered in this work, the  $L$ -shell characteristic radiation from copper is observed. Vacancies in the  $L_I$ ,  $L_{II}$ , and  $L_{III}$  subshells are produced by proton bombardment. The radiation emitted occurs as a result of electrons from the various  $M$  and  $N$  subshells falling into the  $L$ -shell vacancies. In the region of the periodic table near copper, a number of the emission lines have energy greater than the  $L_{III}$  subshell binding energy. This causes a strong attenuation of this group of higher energy lines as compared with those of energy less than the  $L_{III}$  binding energy (mass-absorption jump ratio at  $L_{III}$  edge approximately 5).<sup>10</sup> It was the task of this experiment to isolate these two main com-

ponents and to measure the thick-target yields and the ionization cross section in the  $L_{III}$  shell.

### II. EXPERIMENT

The measured x-ray flux at the surface of the target is the integrated effect of production and self-absorption over the proton path. For a simple case this can be written:

$$I_\mu = n \int_0^{R_0} \exp\left[-\frac{\mu}{\rho}(R_0-r)\right] \omega \sigma_I [E(r)] dr,$$

where  $\mu/\rho$  is in  $\text{cm}^2/\text{g}$ ,  $r$ ,  $R_0$  are in  $\text{g}/\text{cm}^2$ ,  $\sigma_I$  is in  $\text{cm}^2$ . This expression assumes that the total radiation observed comes from the filling of a single shell ionized by the proton. The fluorescent yield ( $\omega$ ) of this shell gives the fraction of vacancies filled by photon emission. The expression also implies that there is one emission line that is absorbed in the target and is characterized by an absorption coefficient ( $\mu$ ).

There are many cases in the  $L$  and  $M$  shells where these simplifying assumptions are not valid. Copper is one of these cases. There are three  $L$  subshells ionized by the protons. In the filling of vacancies in these shells, there are many emission lines of differing energy. As a further complication, some of these emission lines are capable of ionizing, by the photoelectric effect,  $L_{II}$  and  $L_{III}$  shells in other target atoms. Radiation from these shells is small, by virtue of the small fluorescent yield of the  $L$  shell (as extrapolated down from known  $L$ -shell yield values).<sup>11</sup>

The selective self-absorption in the  $L$  shell of the Cu target works to the advantage of the present experiment. All the radiation associated with filling of the  $L_{III}$  shell is below the  $L_{III}$  absorption edge (lowest energy edge). Also, this is the predominant radiation in this group, as compared with the relatively low intensity  $L_{II} \rightarrow M_I$  component (see Ref. 10 and the Appendix of this report). Lines with energy less than the  $L_{III}$  binding energy are:  $L_{III} \rightarrow M_I$ ,  $L_{III} \rightarrow M_{IV}$ ,  $L_{III} \rightarrow M_V$ , and

\* Work performed under the auspices of the U. S. Atomic Energy Commission.

<sup>1</sup> C. Gerthsen and W. Reusse, *Z. Physik* **34**, 478 (1933).

<sup>2</sup> O. Peter, *Ann. Phys. (N. Y.)* **27**, 299 (1936).

<sup>3</sup> M. S. Livingston, F. Genevese, and E. J. Konopinski, *Phys. Rev.* **51**, 835 (1937).

<sup>4</sup> H. W. Lewis, B. E. Simmons, and E. Merzbacher, *Phys. Rev.* **91**, 943 (1953).

<sup>5</sup> P. R. Berington and E. M. Bernstein, *Bull. Am. Phys. Soc.* **1**, 198 (1956).

<sup>6</sup> E. M. Bernstein and H. W. Lewis, *Phys. Rev.* **95**, 83 (1954).

<sup>7</sup> R. C. Jopson, Hans Mark, and C. D. Swift, *Phys. Rev.* **127**, 1612 (1962).

<sup>8</sup> J. M. Khan and D. L. Potter, *Phys. Rev.* **133**, A890 (1964).

<sup>9</sup> E. Merzbacher and H. W. Lewis, *Handbuch der Physik*, edited by S. Flügge (Springer-Verlag Berlin, 1958), Vol. 34, p. 166.

<sup>10</sup> A. H. Compton and S. K. Allison, *X-Rays in Theory and Practice* (D. Van Nostrand Company, Inc., Princeton, New Jersey, 1960).

<sup>11</sup> R. C. Jopson, J. M. Khan, Hans Mark, C. D. Swift, and M. A. Williamson, *Phys. Rev.* **133**, A381 (1964).

$L_{II} \rightarrow M_I$ . This group of lines below the  $L_{III}$  edge can be isolated by the use of Cu absorption foils (see Appendix). It is, therefore, possible to closely approach the conditions implied by the simple yield equation.

It is possible, under these simplifying conditions, to obtain a value for the ionization cross section from this yield equation by differentiation of the expression with respect to the limits of integration<sup>9</sup>  $R_0$ :

$$\omega\sigma_I(E) = -\frac{1}{n} \frac{dI_\mu}{dE} \frac{dE}{dR_0} + \frac{\mu}{n\rho} I_\mu.$$

It is necessary to know the fluorescent yield for the  $L_{III}$  shell, the stopping power of the target for the protons, and the absorption coefficient.

There is one additional complication in the interpretation given above. It is possible to have a redistribution of the initial vacancies among the  $L$  subshells.<sup>12</sup> These Coster-Kronig transitions within the  $L$  shell give up their energy by emission of an electron from the  $M$  or  $N$  shells. It will be shown later that these transitions do not seriously affect the conclusions of the experiment.

### III. EXPERIMENTAL APPARATUS AND METHOD

The experimental apparatus consists of a Cockcroft-Walton linear accelerator, magnetic analyzer, target chamber, absorber foil changer, proportional counter, amplifiers, discriminator, scaler, and pulse-height analyzer (previously described in publication<sup>8</sup>).

The basic analysis employs the observation that there are x-ray emission lines of energy greater than the  $L_{III}$  absorption edge of Cu which are strongly absorbed. Six Cu absorption foils were employed in the experiment (see Table I) as well as one aluminum absorber, in addition to the omnipresent aluminum counter window. The  $(I/I_0)_\alpha^{Cu}$  was measured for foils Cu-A and Cu-C. Together with the measured  $\rho x$  values, this gives a value of  $(\mu/\rho) - 1635$  (60)  $\text{cm}^2/\text{g}$  for this group. From this the  $(I/I_0)_\alpha^{Cu}$  was calculated for the other foils.

*Aluminum foils:*  $Al_1 \equiv Al_2$  (absorbers are identical). The  $(I/I_0)_\alpha^{Al}$  was measured directly, as well as calcu-

lated using the  $\mu/\rho$  value (1440  $\text{cm}^2/\text{g}$ ) of Bearden (private communication)—both were consistent.

$$\left(\frac{I}{I_0}\right)_\alpha^{Al} = 0.0206, \quad \rho x = 2.60 \text{ mg/cm}^2.$$

The following notation will be used:

$I_\alpha^0$ —Total radiation at surface of target of components of energy less than  $L_{III}$  absorption edge.

$I_\beta^0$ —Total radiation measured at surface of target of components of energy greater than  $L_{III}$  edge.

$N_1$ —Total radiation measured with copper foil placed in front of proportional counter.

$N_2$ —Total radiation measured without absorber foils.

$N_3$ —Total radiation measured with aluminum absorber foils.

$(I/I_0)_z^f$ —Transmission of x-ray component “z” by foil “f.”

These can be related by

$$N_1 = I_\alpha^0 \left(\frac{I}{I_0}\right)_\alpha^{Cu} \left(\frac{I}{I_0}\right)_\alpha^{Al_1} + I_\beta^0 \left(\frac{I}{I_0}\right)_\beta^{Cu} \left(\frac{I}{I_0}\right)_\beta^{Al_1},$$

$$N_2 = I_\alpha^0 \left(\frac{I}{I_0}\right)_\alpha^{Al_1} + I_\beta^0 \left(\frac{I}{I_0}\right)_\beta^{Al_1}$$

(proportional counter window only),

$$N_3 = I_\alpha^0 \left(\frac{I}{I_0}\right)_\alpha^{Al_1} \left(\frac{I}{I_0}\right)_\alpha^{Al_2} + I_\beta^0 \left(\frac{I}{I_0}\right)_\beta^{Al_1} \left(\frac{I}{I_0}\right)_\beta^{Al_2}.$$

From these,

$$I_\alpha^0 = N_1 \left[ \left(\frac{I}{I_0}\right)_\alpha^{Cu} \left(\frac{I}{I_0}\right)_\alpha^{Al_1} \right]^{-1},$$

which is the thick Cu-foil relation. (For all Cu foils except Cu-A, the  $\beta$  component is negligible. See Appendix.)

$$\left(\frac{I}{I_0}\right)_\beta^{Al_2} = \frac{N_3 - I_\alpha^0 [(I/I_0)_\alpha^{Al_1} (I/I_0)_\alpha^{Al_2}]}{N_2 - I_\alpha^0 [(I/I_0)_\alpha^{Al_1}]},$$

$$I_\beta^0 = \frac{N_2 - I_\alpha^0 [(I/I_0)_\alpha^{Al_1}]}{(I/I_0)_\beta^{Al_1}}.$$

For the evaluation of these quantities, the independent measurements of  $(I/I_0)_\alpha^{Cu}$  and  $(I/I_0)_\alpha^{Al}$  for the copper and aluminum foils are used.

### IV. INTERPRETATION OF DATA

The primary data obtained in the experiment are the thick-target yields which, together with the experimental and theoretical  $L_{III}$  shell-ionization cross sections, are given in Table II. The low-energy group of

TABLE I. Copper foils.

	$\rho x$ (mg/cm <sup>2</sup> )	$\left(\frac{I}{I_0}\right)_\alpha^{Cu}$
Cu-A	0.26	0.645 -measured
Cu-B	0.82	0.258 -calculated
Cu-C	0.91	0.222 -measured
Cu-D	1.02	0.183 -calculated
Cu-E	2.13	0.0291-calculated <sup>a</sup>
Cu-F	2.40	0.0180-calculated <sup>a</sup>

<sup>a</sup> Exponential law verified for these low transmissions.

<sup>12</sup> E. H. S. Burhop, *The Auger Effect and Other Radiationless Transitions* (Cambridge University Press, Cambridge, 1952).

TABLE II. Thick-target yield and x-ray production cross sections.<sup>a</sup>

$E_p$ (keV)	100	150	200	300	400	500
$I_\alpha^0(\pm 15\%)^b$ $(I_\mu)_\alpha$	$1.9 \times 10^{-5}$	$7.1 \times 10^{-5}$	$1.7 \times 10^{-4}$	$4.8 \times 10^{-4}$	$9.5 \times 10^{-4}$	$1.5 \times 10^{-3}$
$\frac{d(I_\mu)_\alpha}{dE}$	$6.1 \times 10^{-7}$	$1.47 \times 10^{-6}$	$2.4 \times 10^{-6}$	$3.9 \times 10^{-6}$	$5.5 \times 10^{-6}$	$5.4 \times 10^{-6}$
$\frac{dE^c}{d(\rho x)}$	$2.2 \times 10^5$	$2.3 \times 10^5$	$2.2 \times 10^5$	$2.0 \times 10^5$	$1.8 \times 10^5$	$1.70 \times 10^5$
$\frac{1}{n} \frac{d(I_\mu)_\alpha}{dE} \cdot \frac{dE}{d(\rho x)}$	$1.4 \times 10^{-23}$	$3.5 \times 10^{-23}$	$5.6 \times 10^{-23}$	$8.3 \times 10^{-23}$	$1.1 \times 10^{-22}$	$9.7 \times 10^{-23}$
$\frac{1}{n} \frac{\mu}{\rho} (I_\mu)_\alpha$	$3.3 \times 10^{-24}$	$1.24 \times 10^{-23}$	$3.0 \times 10^{-23}$	$8.4 \times 10^{-23}$	$1.66 \times 10^{-22}$	$2.6 \times 10^{-22}$
$\omega_{L_{III}} \sigma_I = \sigma_x$	$1.8 \times 10^{-23}$	$4.74 \times 10^{-23}$	$8.6 \times 10^{-23}$	$1.67 \times 10^{-27}$	$2.73 \times 10^{-22}$	$3.57 \times 10^{-22}$
$\omega_{L_{III}} = 0.05$						
$\sigma_I$ (exp.)	$3.6 \times 10^{-22}$	$9.48 \times 10^{-22}$	$1.92 \times 10^{-21}$	$3.34 \times 10^{-21}$	$5.46 \times 10^{-21}$	$7.14 \times 10^{-21}$
$\sigma_I$ (theoret.) <sup>d</sup>	$1.33 \times 10^{-19}$	...	$1.70 \times 10^{-19}$	$1.72 \times 10^{-19}$	$1.57 \times 10^{-19}$	$1.55 \times 10^{-19}$
$\sigma_{\text{theoret.}} / \sigma_{\text{exp.}}$	370	...	89	51	28	22
$I_\beta^0(\pm 25\%)^b$ $(I_\mu)_\beta$	$1.35 \times 10^{-5}$	$4.4 \times 10^{-5}$	$9.7 \times 10^{-5}$	$2.4 \times 10^{-4}$	$3.6 \times 10^{-4}$	$4.9 \times 10^{-4}$

<sup>a</sup> Units:  $I_\mu$ —x rays per proton;  $dI_\mu/dE$ —x rays per proton per keV;  $dE/d(\rho x)$ —keV per g/cm<sup>2</sup>;  $1/n$ — $1.056 \times 10^{-22}$  g/atom;  $\sigma_x$ —cm<sup>2</sup>.

<sup>b</sup> Ten independent measurements were made at each proton energy—total spread was less than 10%.

<sup>c</sup> S. D. Warshaw and S. K. Allison, Rev. Mod. Phys. 25, 779 (1953).

<sup>d</sup> See Ref. 9.

lines denoted by  $\alpha$  in the notation of this paper originate predominantly from the filling of vacancies in the  $L_{III}$  shell. Employing known values for the stopping power of copper for the protons and the effective  $(\mu/\rho)$  measured, it is possible to obtain the  $L_{III}$ -shell x-ray production cross section, that is, the cross section for the

process of producing x rays originating from the filling of vacancies in the  $L_{III}$  subshell.

The quantity of interest which is to be compared with the Born approximation calculation is the cross section for the process of ionization.<sup>9</sup> On the basis of current understanding of the process, it is believed that the ionization cross section per electron in the  $L$  shell is constant to within 10%, independent of the particular subshell.<sup>9</sup> This leads directly to the fraction of initial vacancies in the  $L_{III}$  subshell—namely,  $\frac{1}{2}$  of the total. It is now necessary to consider the radiationless reorganization within the  $L$  shell.

These Coster-Kronig transitions move vacancies from the more tightly bound levels to less tightly bound levels, with the energy consumed in the ionization of one of the outer, near-valence-level shells. We are concerned with those connecting the  $L_I$  and  $L_{II}$  shells with the  $L_{III}$  shell.

In order to estimate the effectiveness of the Coster-Kronig transitions in enhancing the number of final  $L_{III}$ -shell vacancies over the initial, we must reconsider the thick-target yields. If the ionization cross section per electron is constant, then self-absorption in the target and differences in the subshell fluorescent yields must account for variations in the thick-target yield not attributable to redistribution of initial vacancies. We

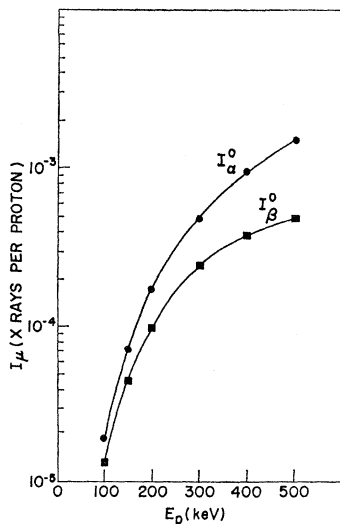


Fig. 1. Copper  $L$ -shell thick-target yields.

observe that the thick-target yields for the  $\alpha$  and  $\beta$  groups approach one another as the proton energy (hence penetration and x-ray self-absorption) decrease. Their ratio decreases from 3 at 500 keV to 1.5 at 100 keV as shown in Fig. 1. They are thus of comparable magnitude and seem to be approaching equality. It is not unreasonable to assume that the subshell fluorescent yields are of comparable magnitude also.<sup>11</sup> The conclusion must be, then, that the Coster-Kronig transitions do not dominate in affecting the intensity distribution.

The final comparison with theory requires a value for the  $L_{III}$  subshell fluorescent yield. This can only be estimated. A value of 0.05 is chosen purely by an argument based upon the energy dependence of the radiative transition probability, choosing a value comparable with that expected from  $K$ -shell data.<sup>11,12</sup>

The comparison with theory in Table I shows a ratio of the theoretical to experimental ionization cross section which takes the value 22 at 500 keV and 370 at 100 keV,<sup>9</sup> This exceeds, by far, the uncertainty associated with the magnitude estimates of fluorescent yields, Coster-Kronig transition probabilities, and variation in ionization cross section. The final conclusion is that the Born approximation calculation needs revision. An alternate approach employs the description of the proton trajectory as a non-straight-line path. The deflected-orbit approach has been employed by Bang and Hansteen for the calculation of the ionization cross section for the  $K$  shell (in this energy range) with great success.<sup>13</sup> It seems desirable to extend this to the  $L$  shell.

#### ACKNOWLEDGMENTS

We would like to express our thanks to Professor Hans Mark, Dr. R. C. Jopson, and C. D. Swift for their time spent in many fruitful discussions. To M. A. Williamson, who produced the absorption foils, we are particularly indebted. A final acknowledgment is extended to R. Cedarlund, F. Stoutamore, and B. Beliz for their assistance in operating the Cockcroft-Walton accelerator.

#### APPENDIX

To test several assumptions in this experiment and to aid in future investigations, an x-ray spectrometer has been constructed which employs a flat potassium-acid-phthalate crystal ( $2d \approx 26.4 \text{ \AA}$ ). The design of the device follows conventional lines and will not be described in detail. A proportional counter is employed to detect the signals, and is useful in monitoring the background. The water-cooled x-ray source (copper target) is run at 1800 V with an electron current of 160 mA, although relative intensity measurements were made between 1100 and 3000 V. The intensity ratios of the Cu  $L$  lines remained constant over this voltage range.

<sup>13</sup> J. Bang and J. M. Hansteen, Kgl. Danske Videnskab. Selskab, Mat. Fys. Medd. 31, No. 13 (1959).

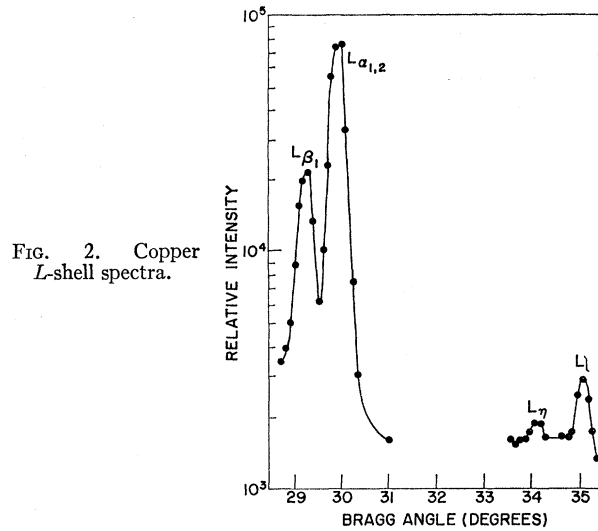


FIG. 2. Copper  $L$ -shell spectra.

It is necessary to verify two statements made in analysis of the experimental data. The first states that the predominant radiation of energy less than the  $L_{III}$  absorption edge originates from the filling of  $L_{III}$ -shell vacancies. The second states that by employing thick ( $\rho x > 0.8 \text{ mg/cm}^2$ ) copper absorbers it is possible to isolate the  $L_{III}$ -shell radiation ( $L_{\alpha_{1,2}}$ , etc.) from the higher energy radiation ( $L_{\beta_1}$ , etc.).

In Fig. 2 are shown the observed lines of energy less than the  $L_{III}$  edge (including  $L_{\beta_1}$  for reference). The transitions are:

$$L_{\beta_1}: L_{II} \rightarrow M_{IV} \text{ (absorbed in } L_{III} \text{ shell),}$$

$$L_{\alpha_{1,2}}: L_{III} \rightarrow M_{IV}, M_V,$$

$$L_{\gamma}: L_{II} \rightarrow M_I,$$

$$L_I: L_{III} \rightarrow M_I.$$

The total intensity associated with the  $L_{\gamma}$  is only a few percent of the total.

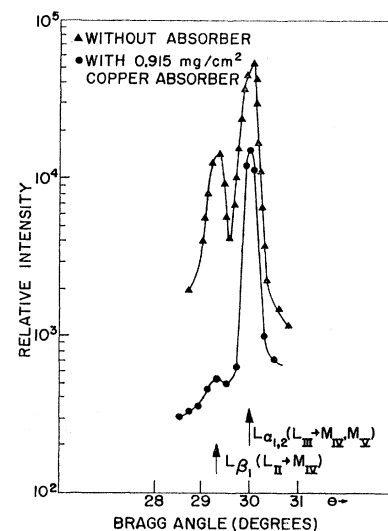


FIG. 3. Copper  $L$ -shell self-absorption.

In Fig. 3 are shown the  $L_{\beta_1}$  and  $L_{\alpha_{1,2}}$  components. The upper curve shows the relative intensities observed in the spectrometer. The lower curve shows the attenuated spectrum when a 0.915-mg/cm<sup>2</sup> copper absorber is placed between the source and crystal. The  $L_{\beta_1}$  component in the attenuated beam represents less than 1% of the total.

It must be accepted that certain reservations must exist in applying the above conclusions to a series of experiments employing the more deeply penetrating protons. At the present time, however, there are no data available regarding relative intensity of lines, etc., originating from proton ionization. Therefore, the electron data must be used as a qualitative reference.

### Theory of Spin-Orbit Coupling in Atoms. III

M. BLUME

*Physics Department, Brookhaven National Laboratory,\* Upton, New York*

A. J. FREEMAN†

*National Magnet Laboratory,‡ Massachusetts Institute of Technology, Cambridge, Massachusetts*

AND

R. E. WATSON

*Bell Telephone Laboratories, Murray Hill, New Jersey*

(Received 26 November 1963)

Spin-orbit coupling constants have been calculated for a number of  $4d$  and  $4f$  shell ions, as well as for some excited states of Li and Cu. The calculations are based on a theory in which the contribution of two-body spin-orbit interactions to the coupling constant is taken into account and exchange effects are included. Fair agreement with experiment is obtained, and several possible reasons for the discrepancies which do occur are discussed. The relation of spin-orbit coupling to hyperfine structure is also considered.

#### I. INTRODUCTION

IN two previous papers,<sup>1</sup> a theory of the spin-orbit coupling constant for many-electron atoms was developed and applied in calculations for a number of the lighter atoms and ions. In the present work, we wish to extend the previous calculations to atoms with unfilled  $4d$  or  $4f$  shells, to consider a number of special cases such as inversion of the  $\text{Cu}(3d)^{10}4f$  doublet and the fine structure of the  $(1s)^22p$ ,  $(1s)^23p$ , and  $(1s)^23d$  states of Li, and to relate these observations to the problem of the calculation of hyperfine structures.

The experimental data available for  $4d$  and  $4f$  shell ions are less accurate and less extensive than was the case for the lighter ions which were considered in II. This makes the task of detailed comparison of our theoretical results with experiment more difficult, but, on the other hand, the importance of theoretical calculation is thereby enhanced, since it will provide added information for use in other work where spin-orbit coupling arises. Using the available experimental data, we find quite good agreement for the theoretical  $4d$

shell results, while the theoretical coupling constants for the rare-earth ions lie somewhat higher than their experimental counterparts. We will compare the rare-earth calculations with those of Ridley,<sup>2</sup> where a use of Hartree functions and the familiar  $\langle(1/r)(\partial V/\partial r)\rangle$  expression for the coupling constant gave good agreement with experiment. The present method starts with a Hartree-Fock (H-F) wave function and properly evaluates the coupling constant for such a function. Since the radial integrals required for the calculation of the coupling constant resemble those used in the calculation of hyperfine interactions (a fact frequently exploited in the past<sup>3-5</sup>), we will estimate from the calculated coupling constants the usefulness of the H-F wave functions for the calculation of hyperfine structure. We shall see that the nonrelativistic  $4d$  and  $4f$  orbitals employed here are more appropriate for the discussion of hyperfine effects than one might have anticipated at first.

We also consider fine-structure doublets because of the historical role they have played in the understanding of spin-orbit coupling. The inadequacy of the standard

\* Work at Brookhaven performed under the auspices of the U. S. Atomic Energy Commission.

† Part of the work of this author was done at the Army Materials Research Agency, Watertown, Massachusetts.

‡ Supported by the U. S. Air Force Office of Scientific Research.

<sup>1</sup> M. Blume and R. E. Watson, *Proc. Roy. Soc. (London)* **A270**, 127 (1962), referred to as Paper I; **A271**, 565 (1963), referred to as Paper II.

<sup>2</sup> E. C. Ridley, *Proc. Cambridge Phil. Soc.* **56**, 41 (1960).

<sup>3</sup> B. R. Judd and I. Lindgren, *Phys. Rev.* **122**, 1802 (1961).

<sup>4</sup> I. Lindgren, *Nucl. Phys.* **32**, 151 (1962).

<sup>5</sup> See, e.g., R. J. Elliott and K. W. H. Stevens, *Proc. Roy. Soc. (London)* **A218**, 553 (1953); **A219**, 387 (1953); and B. Bleaney, *Proc. Phys. Soc. (London)* **A68**, 937 (1955).